Dependency of Jitter Variance on PLL Normalized Noise Bandwidth

Isamu Wakabayashi*, Shun-ichi Urano*, Masatoshi Sano*
*Tokyo University of Science, Faculty of Engineering, Japan
wakaba@ee.kagu.tus.ac.jp

***Abstract*—The present paper describes the dependency of jitter variance on the PLL normalized noise bandwidth, b_L, applying a linearized model of a PLL. The timing circuit consists of a square-law device, a pre-filter, and a PLL arranged in tandem. The transmission systems are PAM, ASK, and QAM for a root roll-off bandlimiting scheme. An additive white Gaussian noise exists at the receive filter input. The pre-filter and PLL are referred to as the extractor.**

The SN and NN components of jitter variance are proportional to b_L, whereas the SS component is proportional to the square of b_L. The mechanism of this discrepancy is clarified through a detailed discussion of the relationships among the jitter source PSD, the extractor transfer function characteristics, and the jitter PSD. This proportional relation holds for any transmission system, any SNR, and any roll-off factor considered herein.

Keywords*— *jitter variance, PLL, PAM, ASK, QAM

I. Introduction

The present paper describes the dependency of jitter variance on a phase locked loop (PLL) normalized noise bandwidth in order to clarify the jitter performance of the timing circuit. In order to evaluate the jitter generation and the jitter performance of the timing circuit, it is important to determine the jitter power spectral density (jitter PSD).

The self-noise in-phase and quadrature power spectra at the output of a nonlinear (NL) device in the case of a timing circuit with a squarer [1] or with any even high-order NL device [2] are obtained assuming a high signal-to-noise ratio (SNR) for a baseband PAM system. In a properly designed synchronizer, only the quadrature component contributes to timing jitter [3]. At the low SNR for linear modulations, a timing extraction algorithm denoted as the Square-Law Nonlinearity (SLN) is provided based on maximum likelihood estimation [4]. Low SNR operation is performed according to the circumstances. In [5], timing jitter for PAM, ASK, and QAM in an arbitrary SNR is analyzed in an arbitrary band-limiting scheme. An additive white Gaussian noise is assumed to exist at the receive filter input, and the timing circuit consists of a square-law device, a pre-filter, and a PLL arranged in tandem. A closed-form representation of the jitter PSD at the PLL output is derived and expressed as an arbitrary transmit pulse waveform, an arbitrary receive filter transfer function, and an arbitrary SNR. The pre-filter and PLL are hereinafter referred to as the extractor. The jitter PSD is represented by a linear combination of the jitter source PSD at the squarer output and the extractor transfer function characteristics.

The jitter PSD has SS, SN, and NN components. Each component of jitter variance can be calculated by integrating the corresponding component of jitter PSD over a finite frequency domain. The SS component is obtained as the cross product of the signal itself and is often referred to as self-noise or pattern jitter [3]. The SN component is obtained as the cross product of the signal and the noise. The NN component is obtained as the cross product of the noise itself. The total jitter variance is obtained as the sum of these three components.

As a typical application of the closed-form representation, the jitter variance is calculated for a cosine roll-off band-limiting scheme. Jitter dependencies on system parameters, i.e., SNR: ρ; alphabet size: M; transmission scheme; PLL normalized noise bandwidth: b_L; and roll-off factor: α, have been presented [6]. However, the jitter dependency on b_L has not yet been clarified or discussed in detail. Therefore, we deal with this subject in the present paper.

The jitter variances of the SN and NN components are proportional to the PLL normalized noise bandwidth, b_L, whereas the SS component is proportional to the square of b_L. This result is rather general and is applicable to any transmission system, any SNR, and any roll-off factor considered in the present paper. Thus, it is important to clarify the discrepancy mechanism in the proportional relation through a detailed examination of the relationships among the jitter source PSD, the extractor transfer function characteristics, and the jitter PSD.

II. Assumption

A. Receiver Configuration and Parameters

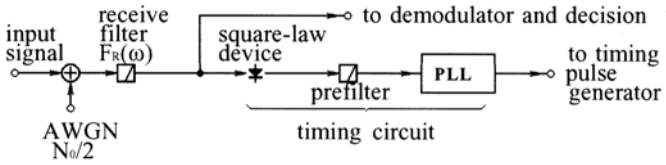

Figure 1. Receiver configuration

Figure 1 shows the receiver configuration. The timing circuit consists of a square law device, a pre-filter, and a PLL in tandem. Additive white Gaussian noise is applied at the receive filter input. The pre-filter transfer function is assumed to be unity here. The PLL is assumed to be of second-order, and the loop filter consists of an active filter. A typical value of PLL damping factor ζ is $1/\sqrt{2}$, and its normalized noise bandwidth $b_L (= B_L T = 2\pi B_L/\omega_r)$ ranges from 10^{-4} to 10^{-2}. Here, B_L is the noise bandwidth, which is a measure of the PLL bandwidth [7]. In addition, T is the symbol period, and ω_r is the clock radian frequency. Typical transmission systems include PAM, ASK, and QAM. The root roll-off band limitation [8] is applied, and the roll-off factor ranges from 0.1 to 1.0. The SNR, ρ, at the timing circuit input ranges from 0 to 40 dB. The transmit data sequence, a_n, in PAM and ASK and the data sequences, a_n and b_n, in QAM take i.i.d. random variables:

$$-(M\text{-}1), -(M\text{-}3), \cdots, -3, -1, 1, 3, \cdots, M\text{-}3, M\text{-}1,$$

where M is an even number and is referred to as the alphabet size. Thus, the second-order moment M_2 and the fourth-order moment M_4 for the data sequences can be given, respectively, as follows:

$$M_2 = E[a_n^2] = E[b_n^2] = (M^2 - 1)/3 \quad (1)$$

$$M_4 = E[a_n^4] = E[b_n^4] = (M^2 - 1)(3M^2 - 7)/15 \quad (2)$$

B. Extractor Transfer Function Characteristic

The pre-filter and PLL are referred to as the extractor. Here, the pre-filter transfer function is assumed to be unity for simplicity. Thus, the timing extractor transfer function $H_k(\omega)$ in [5] becomes the PLL transfer function. The pre-filter is expected to be useful as a self-noise reduction technique [9]. The effect of the pre-filter on timing jitter is a future subject.

The PLL closed-loop transfer function is expressed as follows:

$$H(\omega) = \frac{\omega_n^2 + j2\zeta\omega_n\omega}{\omega_n^2 - \omega^2 + j2\zeta\omega_n\omega} \quad (3)$$

where ω_n is a natural frequency, and ζ is a damping factor [7]. The term $|H(\omega)|^2$ is given by

$$|H(\omega)|^2 = \frac{1 + 4\zeta^2\omega^2\omega_n^{-2}}{(1 - \omega^2\omega_n^{-2})^2 + 4\zeta^2\omega^2\omega_n^{-2}} \quad (4)$$

The PLL one-sided noise bandwidth B_L is given by

$$B_L = \frac{1}{2\pi}\int_0^\infty |H(\omega)|^2 \, d\omega = \frac{\omega_n}{2}\left(\zeta + \frac{1}{4\zeta}\right) \quad (5)$$

In the present paper, the normalized noise bandwidth b_L is defined as follows:

$$b_L = B_L T = 2\pi B_L/\omega_r \quad (6)$$

Thus, the PLL transfer function characteristic is given by

$$|H(\omega)|^2 = \frac{1 + (9/4)\pi^2 b_L^{-2}(\omega/\omega_r)^2}{1 + (9/8)^2\pi^4 b_L^{-4}(\omega/\omega_r)^4} \quad (7)$$

The extractor transfer function in [5] can be expressed as follows;

$$H_k(\omega) = |H(\omega)|^2 \quad ; k = 1,2,3,4 \quad (8)$$

III. Representations of Jitter PSD and Jitter Source PSD

General equations for jitter PSD, the extractor transfer function, and jitter source PSD are shown in [5]. We arrange these equations in order to satisfy the assumptions. Then, the arranged equations for jitter PSD and jitter source PSD are represented in normalized form in order to discuss the jitter performance.

A. Basic Parameters

Since the pre-filter transfer function is assumed to be unity, coefficients of C_T, θ_T, and D_2 in [5] can be expressed as follows;

$$\begin{aligned} C_T &= A(\omega_r) = 1 \\ \theta_T &= \angle A(\omega_r) = 0 \\ D_2 &= \exp(j2\theta_T) = 1 \end{aligned} \quad (9)$$

where $A(\omega)$ is the pre-filter transfer function.

Since the cosine roll-off bandlimiting scheme is assumed, coefficients of A_T, ϕ_T, D_1 and β in [5] can be expressed as follows;

$$\begin{aligned} A_T &= |G_a(\omega_r)| = \alpha/8T \\ \phi_T &= \angle G_a(\omega_r) = 0 \\ D_1 &= \exp(j2\phi_T) \\ \beta &= 1 - \alpha/4 \end{aligned} \quad (10)$$

where $G_a(\omega)$ is the frequency spectrum of $g^2(t)$, and $g(t)$ is the pulse waveform at the receive filter output.

B. Jitter PSD, Jitter Source PSD and Normalization

The SS, SN, and NN components for the jitter PSD can be given as follows;

$$W_{\phi SS}(\omega) = |H(\omega)|^2 \left\{C_{SS}^{(1)}G_1(\omega) + C_{SS}^{(2)}G_2(\omega)\right\} \quad (11)$$

$$W_{\phi SN}(\omega) = |H(\omega)|^2 \, C_{SN}\rho^{-1}G_3(\omega) \quad (12)$$

$$W_{\phi NN}(\omega) = |H(\omega)|^2 \, C_{NN}\rho^{-2}G_4(\omega) \quad (13)$$

where ρ is the SNR at the receive filter output. The jitter source PSD, i.e., $G_1(\omega)$, $G_2(\omega)$, $G_3(\omega)$, and $G_4(\omega)$, can be expressed in the following equations;

$$\begin{aligned} G_1(\omega) = \frac{1}{4\pi A_T^2}\Bigg[& \int_{-\infty}^{\infty} G^2(x)\Big(G^2(x-\omega+\omega_r) + G^2(x-\omega-\omega_r)\Big)dx \\ & + \int_{-\infty}^{\infty} G(x)G(x-\omega)\big\{G(x+\omega_r)G(x-\omega-\omega_r) \\ & \qquad + G(x-\omega_r)G(x-\omega+\omega_r)\big\}dx \\ & - \int_{-\infty}^{\infty} G(x)G(x-\omega)\big\{G(x+\omega_r)G(x-\omega+\omega_r) \\ & \qquad + G(x-\omega_r)G(x-\omega-\omega_r)\big\}dx \\ & + \int_{-\infty}^{\infty} G(x)G(x+\omega_r)G(x-\omega+\omega_r)G(x-\omega+2\omega_r)dx \\ & + \int_{-\infty}^{\infty} G(x)G(x-\omega_r)G(x-\omega-\omega_r)\,G(x-\omega-2\omega_r)dx\Bigg] \end{aligned} \quad (14)$$

$$G_2(\omega) = -\frac{T}{2A_T^2}\{G_a(\omega-\omega_r) - G_a(\omega+\omega_r)\}^2 \quad (15)$$

$$G_3(\omega) = \frac{\beta}{2\pi A_T^2}\int_{-\infty}^{\infty} G^2(x)\{G(x-\omega+\omega_r) + G(x-\omega-\omega_r)\}dx \quad (16)$$

$$G_4(\omega) = \frac{\beta^2}{2A_T^2}\{G_a(\omega-\omega_r) + G_a(\omega+\omega_r)\} \quad (17)$$

where $G_1(\omega)$, $G_2(\omega)$, $G_3(\omega)$, and $G_4(\omega)$ can be proven to be even functions with respect to ω. The integrand $G(\omega)$ is given by $G_T(\omega)\cdot G_R(\omega)$. $G_T(\omega)$ and $G_R(\omega)$ are, respectively, the frequency spectrum of a transmitted pulse waveform and the transfer function of the receive filter. Each of these terms is assumed to be the root roll-off characteristics. $G_R(\omega)$ is the equivalent low pass transfer function of

$F_R(\omega)$ in Figure 1. The coefficients; $C_{SS}^{(1)}$, $C_{SS}^{(2)}$, C_{SN}, and C_{NN} in (11), (12), and (13) are determined by the transmission scheme. In QAM, these coefficients are given as follows [5];

$$C_{SS}^{(1)} = \frac{1}{2}, C_{SS}^{(2)} = \frac{1}{4}(3 - M_2^{-2} M_4), C_{SN} = \frac{1}{2}, C_{NN} = \frac{1}{2} \quad (18)$$

where M_2 and M_4 are the second-order moment and fourth-order moment of modulation data as given by (1) and (2), respectively.
In 16QAM, the coefficients are obtained as follows;

$$C_{SS}^{(1)} = 1/2, C_{SS}^{(2)} = 0.34, C_{SN} = 1/2, C_{NN} = 1/2 \quad (19)$$

C. Normalized Jitter PSD and Jitter Source PSD

The normalized jitter PSDs, $K_{SS}(\Omega\omega_r)$, $K_{SN}(\Omega\omega_r)$, and $K_{NN}(\Omega\omega_r)$, are defined as follows;

$$K_{SS}(\Omega\omega_r) = \alpha^2 T^{-1} W_{\phi SS}(\Omega\omega_r) \quad (20)$$

$$K_{SN}(\Omega\omega_r) = \alpha^2 T^{-1} W_{\phi SN}(\Omega\omega_r) \quad (21)$$

$$K_{NN}(\Omega\omega_r) = \alpha^2 T^{-1} W_{\phi NN}(\Omega\omega_r) \quad (22)$$

where $\Omega (= \omega/\omega_r)$ is referred to as the normalized frequency.

The normalized jitter source PSDs, $G_{SS}(\Omega\omega_r)$, $G_{SN}(\Omega\omega_r)$, and $G_{NN}(\Omega\omega_r)$, are defined as follows;

$$G_{SS}(\Omega\omega_r) = \alpha^2 T^{-1} \left\{ C_{SS}^{(1)} G_1(\Omega\omega_r) + C_{SS}^{(2)} G_2(\Omega\omega_r) \right\} \quad (23)$$

$$G_{SN}(\Omega\omega_r) = C_{SN} \rho^{-1} \alpha^2 T^{-1} G_3(\Omega\omega_r) \quad (24)$$

$$G_{NN}(\Omega\omega_r) = C_{NN} \rho^{-2} \alpha^2 T^{-1} G_4(\Omega\omega_r) \quad (25)$$

Thus, the following equations of jitter PSD are obtained;

$$K_{SS}(\Omega\omega_r) = |H(\Omega\omega_r)|^2 G_{SS}(\Omega\omega_r) \quad (26)$$

$$K_{SN}(\Omega\omega_r) = |H(\Omega\omega_r)|^2 G_{SN}(\Omega\omega_r) \quad (27)$$

$$K_{NN}(\Omega\omega_r) = |H(\Omega\omega_r)|^2 G_{NN}(\Omega\omega_r) \quad (28)$$

These equations are not dependent on ω_r and are hereinafter used in order to discuss the jitter performance of the timing circuit.

D. Jitter Variance and its Three Components

The total jitter variance σ_ϕ^2 and its three components are given, respectively, by the following equations:

$$\sigma_\phi^2 = \sigma_{\phi SS}^2 + \sigma_{\phi SN}^2 + \sigma_{\phi NN}^2 \quad (29)$$

$$\sigma_{\phi SS}^2 = \frac{1}{\alpha^2} \int_{-\infty}^{\infty} K_{SS}(\Omega\omega_r) d\Omega \quad (30)$$

$$\sigma_{\phi SN}^2 = \frac{1}{\alpha^2} \int_{-\infty}^{\infty} K_{SN}(\Omega\omega_r) d\Omega \quad (31)$$

$$\sigma_{\phi NN}^2 = \frac{1}{\alpha^2} \int_{-\infty}^{\infty} K_{NN}(\Omega\omega_r) d\Omega \quad (32)$$

IV. NUMERICAL RESULTS and DISCUSSION

A. Dependency of Jitter Variance on PLL Bandwidth

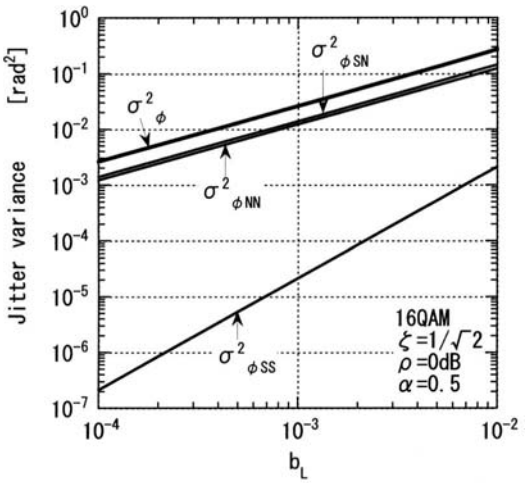

(a) SNR = 0 dB

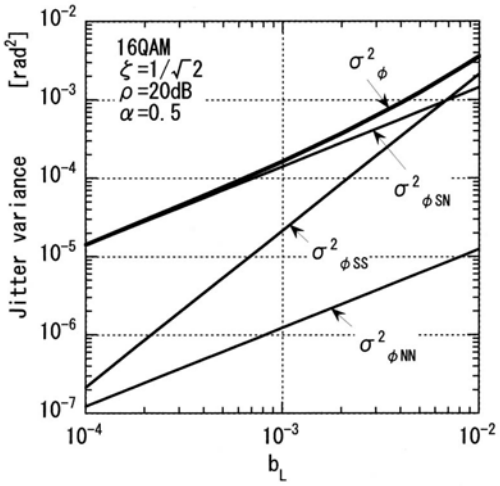

(b) SNR = 20 dB

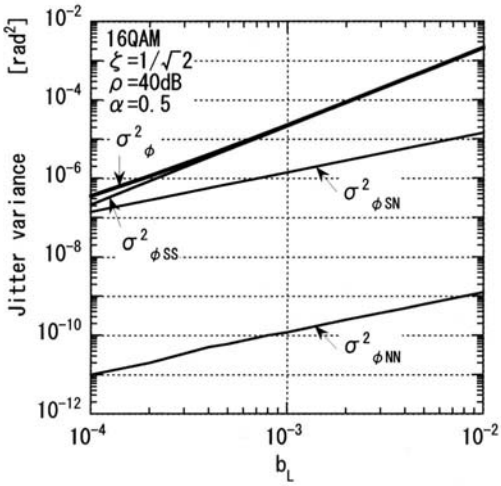

(c) SNR = 40 dB

Figure 2. Dependency of jitter variance on PLL normalized noise bandwidth b_L

Figure 2 shows examples of the numerical results that demonstrate the dependency of jitter variance on the PLL normalized noise bandwidth with SNRs of 0, 20, and 40 dB. The horizontal axis is the PLL normalized noise bandwidth b_L ($b_L = B_L T$). The transmission scheme is 16QAM with a roll-off factor of 0.5.

The SN ($\sigma^2_{\phi SN}$) and NN ($\sigma^2_{\phi NN}$) components of jitter variances are proportional to b_L, whereas the SS ($\sigma^2_{\phi SS}$) component is proportional to the square of b_L. This is the first time that the jitter dependency on b_L has been shown in terms of SS, SN, and NN components. These performances hold for any SNR, any transmission scheme, and any roll-off factor considered in the present paper. This may be considered to be due to the relationships between the jitter source PSD, the extractor transfer function characteristics, and the jitter PSD.

Figure 2(a) shows that the total jitter variance (σ^2_{ϕ}) is proportional to b_L because the SN and NN components are dominant. Figure 2(b) shows that, on the whole, σ^2_{ϕ} is proportional to b_L, because the SN component is dominant. Figure 2(c) shows that σ^2_{ϕ} is proportional to the square of b_L because the SS component is dominant.

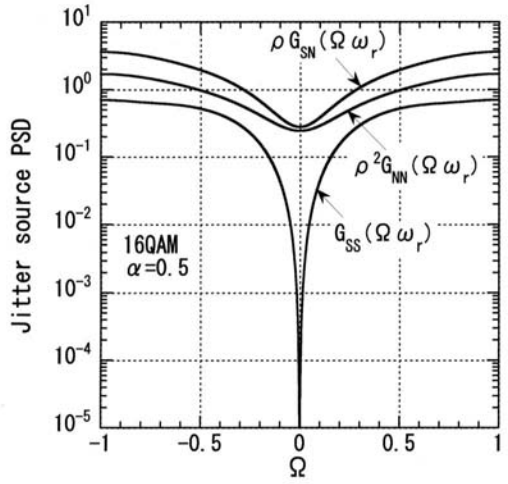

Figure 3. Normalized jitter source PSD at PLL input

B. Discussion of the Dependency

The normalized jitter PSD is given as the product of the normalized jitter source PSD and the PLL transfer function characteristics, as given in (26), (27), and (28). The jitter variance can be obtained by frequency integration of the normalized jitter PSD, as given in (30), (31), and (32). The dependency of jitter variance on the PLL normalized noise bandwidth b_L is discussed in this section in terms of the relationships among the normalized jitter source PSD, the PLL transfer function characteristics, and the normalized jitter PSD.

1) Jitter Source PSD:

Figure 3 shows examples for the numerical results of the normalized jitter source PSD. The horizontal axis represents the normalized frequency Ω. The transmission scheme is 16QAM with a roll-off factor of 0.5.

The SS component exhibits a sharp dip in the vicinity of $\Omega = 0$, specifically. The SN and NN components exhibit comparatively flat characteristics. These characteristics are symmetric with respect to $\Omega = 0$. The mutual relationship among these three components does not change, even when the alphabet sizes, transmission schemes, and roll-off factors vary, because the characteristics are determined by (23), (24), and (25).

2) PLL Characteristics:

Figure 4 shows the numerical results for the PLL closed-loop transfer function characteristics calculated from (7). Figure 4(a) shows the wideband characteristics when b_L ranges from 10^{-3} to 10^{-2}, and Figure 4(b) shows the narrowband characteristics for a b_L of 10^{-3}.

3) SS Component of Normalized Jitter PSD:

Figure 5 shows examples of the SS component of the normalized jitter PSD at the PLL output. The vertical axis represents $K_{SS}(\Omega\omega_r)$, and the horizontal axis represents the normalized frequency Ω. The transmission scheme is 16QAM with a roll-off factor of 0.5. The PLL normalized noise bandwidth b_L ranges from 10^{-3} to 10^{-2}.

Since the SS component of jitter source PSD exhibits a sharp dip

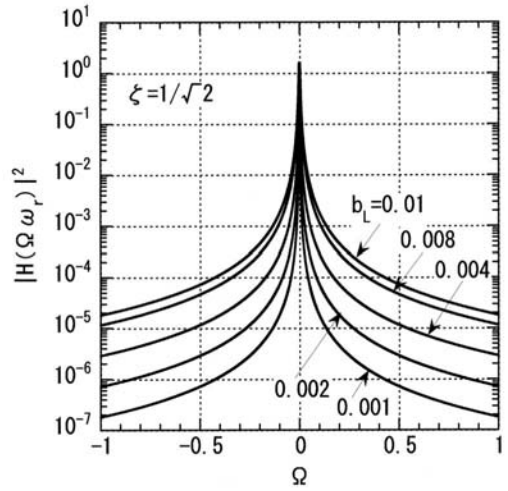

(a) Wideband characteristics

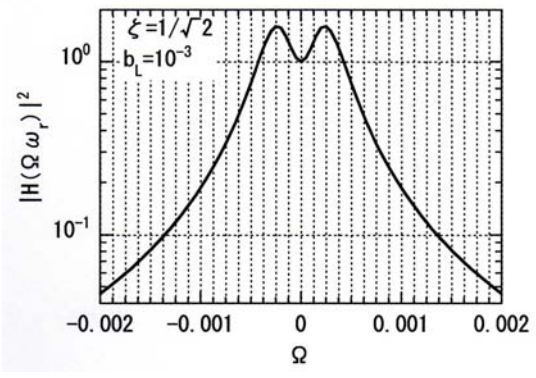

(b) Narrowband characteristic

Figure 4. PLL closed loop transfer function characteristics

in the vicinity of $\Omega = 0$ within the PLL bandwidth, the narrowband bandlimiting effect of PLL is insufficient. Therefore, the SS component of the jitter PSD is to be determined by the wide band characteristics of both the jitter source PSD and the PLL closed-loop transfer function characteristics. The distribution of the SS component of the jitter PSD with each b_L exhibits a similar shape and the jitter PSD amplitude increases or decreases in proportion to the square of b_L. The jitter variance is given by the frequency integration of the jitter PSD. Thus, the SS component of the jitter variance ($\sigma^2_{\varphi SS}$) is proportional to the square of b_L. This relation holds for any b_L ranging from 10^{-4} to 10^{-3}.

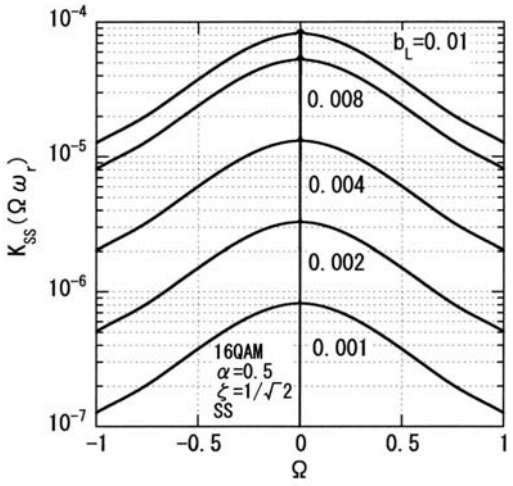

Figure 5. SS component of normalized jitter PSD

4) SN Component of Normalized Jitter PSD:

Figure 6 shows examples of the SN component of the normalized jitter source PSD, the PLL transfer function characteristics, and the normalized jitter PSD. The horizontal axis is a logarithmic scale in order to enlarge the narrowband characteristics.

In this case, since the SN component of the jitter source PSD exhibits almost flat characteristics within the PLL bandwidth, the narrowband bandlimiting effect of the PLL functions sufficiently well. The SN component of the jitter PSD exhibits a shape that is similar to the PLL characteristics. The bandwidth of the jitter PSD for each b_L becomes narrower or wider in proportion to b_L. The jitter variance is given by the frequency integration of the jitter PSD. Thus, the SN component of the jitter variance is proportional to b_L. This relation also holds for any b_L in the range from 10^{-4} to 10^{-3}.

5) NN Component of Normalized Jitter PSD:

Figure 7 shows examples of the NN component of the normalized jitter source PSD and the normalized jitter PSD. The PLL transfer function characteristics are the same as those in Fig. 6(b). Thus, similar to the discussion of the SN component, the NN component of jitter variance is proportional to b_L. This relation also holds for any b_L in the range from 10^{-4} to 10^{-3}.

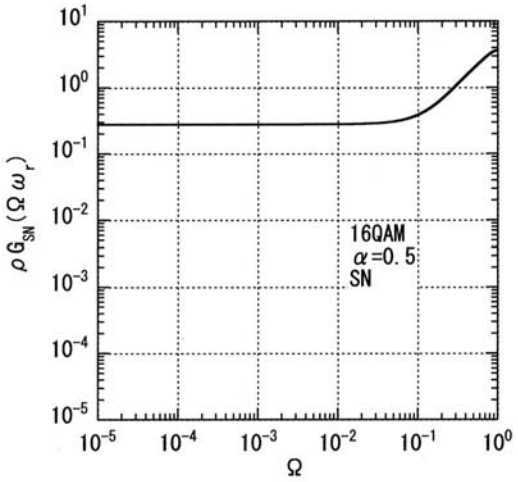

(a) SN component of normalized jitter source PSD

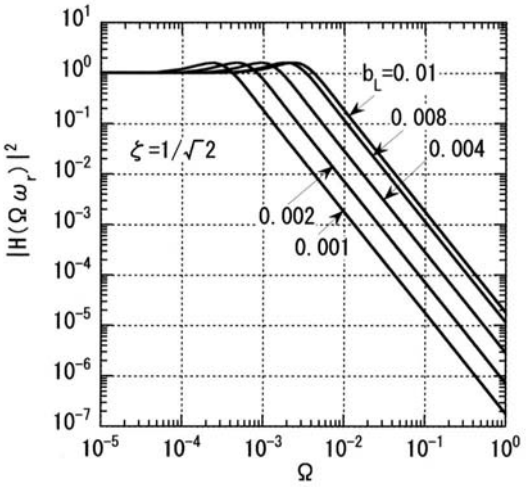

(b) PLL characteristics

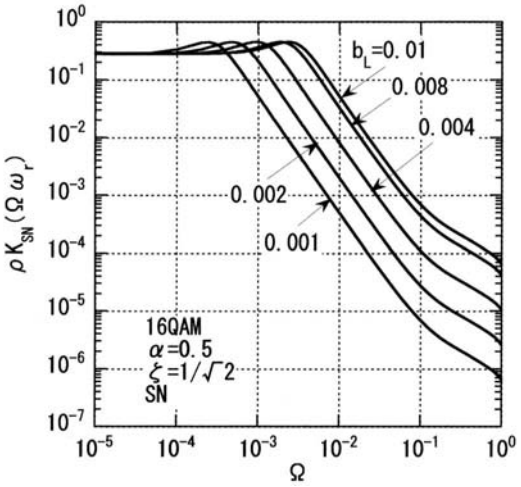

(c) SN component of normalized jitter PSD

Figure 6. Spectral characteristics of SN component and PLL

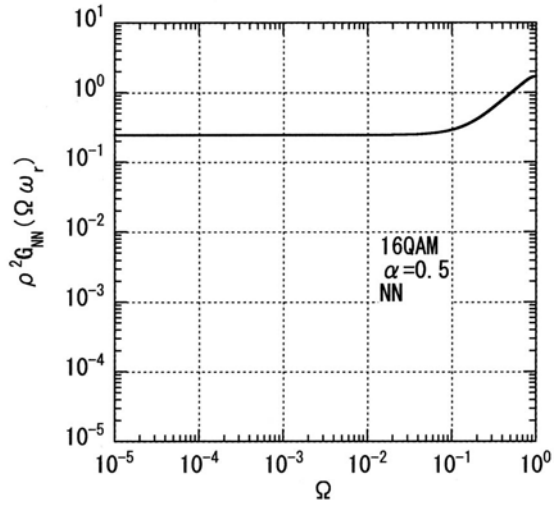

(a) NN component of normalized jitter source PSD

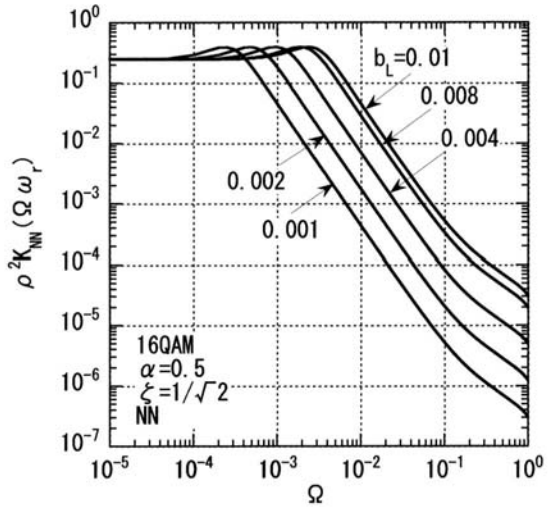

(b) NN component of normalized jitter PSD

Figure 7. Spectral characteristics of NN component

V. CONCLUSION

The dependency of jitter variance and its three components on the PLL normalized noise bandwidth, b_L, has been demonstrated, applying a linearized model of a PLL. The PLL is assumed to be of second-order and the loop filter consists of an active filter.

The SN and NN components of jitter variance are proportional to b_L, whereas the SS component is proportional to the square of b_L. This discrepancy mechanism is clarified through the detailed examination in terms of the relationships among the jitter source PSD, the PLL transfer function characteristics, and the jitter PSD.

This result is rather general and is applicable to any transmission system, any SNR, and any roll-off factor considered in the present paper.

The pre-filter transfer function is assumed to be unity here for simplicity. But, the pre-filter is expected to be useful for self-noise (SS component) reduction techniques. Therefore, we intend to discuss the effect of the pre-filter on timing jitter. In addition, the effect of timing jitter on the symbol error rate will be discussed in the future subject.

ACKNOWLEDGMENT

The authors would like to thank Professor Kazuhiro Miyauchi for his valuable guidance and suggestions.

REFERENCES

[1] T. T. Fang, "I and Q decomposition of self-noise in square-law clock regenerators," *IEEE Trans. Commun.*, vol.COM-36, no.9, pp.1044-1052, September 1988.

[2] Erdal Panayırcı, "Analysis of self-noise in a clock recovery system with a high-order nonlinearity," *IEEE Trans. Information*, vol.49, no.11, pp.3106-3116, November 2003.

[3] F. M. Gardner, "Self-noise in synchronizer," *IEEE Trans. Commun.*, vol.COM-28, no.8, pp.1159-1163, Aug. 1980.

[4] José A. López-Salcede and Gregori Vázquez, "Asymptotic equivalence between the unconditional maximum likelihood and the square-law nonlinearity symbol timing estimation," *IEEE Trans. Signal Processing*, vol.54, no.1, pp.244-257, Jan. 2006.

[5] Kazuhiro Miyauchi, Isamu Wakabayashi, "Analysis of timing jitter in PAM, ASK and QAM," *IEICE Trans. Commun. (Japanese ed.)*, vol.J93-B, no.8, pp.1051-1060, Aug. 2010.

[6] Isamu Wakabayashi, "Timing jitter in PAM, ASK, and QAM for a bandlimiting scheme," *12th Proceedings of ICACT 2010*, vol.1, pp.318-323, Feb. 2010.

[7] Floyd M. Gardner, *Phaselock Techniques*, Third Ed., pp.129-130, A John Wiley & Sons, Inc., 2005.

[8] Kazuhiro Miyauchi, Isamu Wakabayashi, *An Introduction to Digital Communication Theory*, pp.47-61, CORONA PUBLISHING Co. Ltd., September 2005.

[9] Dongmin Lim, "A modified Gardner detector for symbol timing recovery of M-PSK signals," *IEEE Trans. Commun.*, vol.52, no.10, pp.1643-1647, October 2004.